Reinvestigation of the Gas-Phase Structure of RDX Using Density Functional Theory Predictions of Electron-Scattering Intensities

Theodore Vladimiroff

Warheads, Energetics and Combat-Support Armaments Center, U. S. Army TACOM-ARDEC, Picatinny Arsenal, New Jersey 07806-5000

Betsy M. Rice*

U.S. Army Research Laboratory, AMSRL-WM-BD, Aberdeen Proving Ground, Maryland 21005-5066

Received: June 19, 2002; In Final Form: August 20, 2002

Density functional calculations at the B3LYP/6-31G* level are used to generate electron-diffraction intensity curves for six conformers of hexahydro-1,3,5-trinitro-*s*-triazine (RDX). These are compared with an experimental curve (Shishkov, I. F.; Vilkov, L. V.; Lolonits, M.; Rozsondai, B. *Struct. Chem.* **1991**, *2*, 57) for which a structural model of gas-phase RDX was proposed. The calculations were done to investigate possible causes of the discrepancies between the theoretical structures and the molecular model proposed by Shishkov et al. The results show that alternative structures to that proposed from experiment can reproduce the measured intensities. Also, barriers to interconversion between the conformers were calculated to investigate the possibility of rapid interconversion at the temperature of the experiment (433 K). Barriers range from 1.5 to 5 kcal/mol, suggesting that measurements of RDX in the gas phase might reflect a dynamically averaged structure that represents contributions from the individual conformers.

Introduction

One of the methods by which the structure of a molecule in the gas phase can be determined is through the use of electron diffraction. Diffracted intensities measured from electron-scattering experiments depend on all of the interatomic distances in the molecule, and thus information about a molecular structure can be gained from these measurements. This method of structural determination works well for small molecules. Larger molecules, however, often have many interatomic distances of almost equal magnitudes, thus making it difficult to resolve all of them. Also, a large molecule is more likely to exist in more than one conformation in the gas phase. Ideally, ab initio theory should be used to augment experimental interpretation of gas-phase electron diffraction (GED) experiments.[1] However, it has only been recently that reliable theoretical predictions could be made for large polyatomic molecules. When reliable theoretical information was not available, experimentalists were forced to follow an alternative procedure in interpreting the results of GED experiments. The procedure consists of making assumptions about the molecular structure, developing a molecular model based on those assumptions, parametrizing the structural variables using information from similar molecules, and then refining the parameters so that the simulated diffraction intensities are a good fit to the experimental spectra. Sometimes this procedure leads to discrepancies between theory and experiment. The system that is the focus of this study, hexahydro-1,3,5-trinitro-*s*-triazine (RDX), provides such an example. For RDX, there are notable structural discrepancies between ab initio[2,3] and experimental[4] values. An earlier theoretical study[3] suggested that the discrepancies might be due to structural assumptions used by the experimentalists in developing molecular models whose simulated electron diffraction spectra agreed with measured intensities. This hypothesis provided the motivation for this study in which electron-scattering curves are calculated using the quantum-mechanically predicted structures for direct comparison with the experimental intensities. In this work, we present the results of such calculations. Section II is a review of earlier theoretical and experimental structural studies that led to this investigation, and section III is a description of how structural information is used to generate electron diffraction spectra. Section IV will provide details of other quantum mechanical calculations performed for this study. Section V provides a discussion of the results and is followed by the conclusions in section VI.

Previous Experimental and Theoretical Structural Studies for RDX

The structure of RDX at ambient conditions is in the α-crystalline form and has been well established from X-ray[5] and neutron diffraction[6] experiments. The structures of RDX in solution, in the vapor phase, and in the less-stable β solid form are not as well established. Various experimental techniques have been used in order to determine the structure of RDX in the gas and liquid states. Filhol et al.[7] observed only one line in the proton NMR spectra of RDX in solution. Karpowicz and Brill[8] also observed only a sharp singlet in the 360-MHz NMR spectrum of RDX at −80 °C. These observations can be explained only on the basis of an RDX structure in which the two methylene protons are equivalent or the protons are effectively being averaged to be the same on the time scale of the NMR experiment by a rapid interconversion of several different structures. Several groups[7−9] of investigators have obtained infrared spectra of RDX in the solid state and in

* Corresponding author. E-mail: betsyr@arl.army.mil.

10.1021/jp021450b CCC: $22.00
Published on Web 09/28/2002

solution. Karpowicz and Brill[8] supplemented these data by obtaining Fourier transform infrared spectra of RDX in the vapor state. The interpretations of all these data are quite similar. RDX in the α crystal is in the chair conformation with one nitro group in the equatorial (E) position and two nitro groups in the axial (A) position (AAE). The site symmetry is C_1, but the molecule almost possesses a plane of symmetry determined by one of the methylene groups and the N−N bond on the opposite end of the molecule. All of the infrared spectra of RDX in solution, in the β solid, and in the gas phase are remarkably similar in that some of the fine structure observed in the α solid phase is lost. This suggests that some of the bands observed in the α solid phase collapse into single, doubly degenerate vibrations because of higher symmetry. Furthermore, the analysis suggests that RDX has essentially C_{3v} symmetry in the β state, in the gas phase, and in solution, but the results could not provide more detailed descriptions of the molecular structure.[8] Also, this study could not conclusively establish whether the results are due to a single structure with C_{3v} symmetry or whether a large amount of conformational flexibility of the NO_2 groups and the ring produces a conformationally averaged structure with C_{3v} symmetry.[8]

After the Karpowicz and Brill study, Shishkov et al.[4] conducted electron-scattering experiments on RDX in the gas phase. Molecular models were used to generate simulated diffraction intensities for comparison with experiment in order to extract structural parameters. Both the boat and the chair forms of RDX were considered with all of the nitro groups in either axial or equatorial positions. Simulated molecular intensities were found to be in the best agreement with experiment by assuming a model structure of RDX in the chair form with all of the nitro groups in axial positions (AAA). This conformer was chosen for further refinement, and structural parameters and mean-square amplitudes (MSAs) of vibration (both required for generating the intensities) were simultaneously varied in a least-squares fitting procedure to produce a model whose simulated electron-diffraction spectrum best matched experiment.

Two density functional theory (DFT) studies of RDX have been published,[2,3] one of which showed that DFT geometries and simulated infrared spectra are in as good or better agreement with experiment than second-order Moeller−Plesset (MP2) calculations.[3] In these works, local energy minima were found that correspond to chair conformers with different arrangements of the NO_2 groups relative to the ring: AAA,[2,3] AAE,[2,3] EEA,[2] and EEE.[3] A twisted and a boat conformer were also identified[2] and will be denoted hereafter as "twist" and "boat". The differences in energies of all but one of these conformers are quite small (∼1 kcal/mol).[2,3] Only the EEE conformer was found to be significantly higher in energy (∼5 kcal/mol[3]). Comparison of the AAE conformer to the experimental structure showed good agreement.[2,3] However, when the theoretical structure for the AAA conformer was compared with the gas-phase geometry proposed by Shishkov et al.,[4] two significant differences in the molecular structures were evident: first, a large deviation in the C−N−C ring angle was noted. The predicted value for this angle is 115.6° at the B3LYP/6-31G* level of theory[2,3] whereas the experimental value[4] is 123.7°. This seems like a rather large deviation because theoretical predictions of these angles (115.0, 115.4, and 115.5°) for the chair (AAE) structure are within one degree of the experimental measurements (115.1, 114.6, and 114.8°) of crystalline RDX,[6] even though the experimental values include crystal-field effects. We would expect the same degree of accuracy for the AAA gas-phase structure. In Shishkov et al., [4] it is suggested that the large difference in the CNC angles between the gas-phase structure and the α solid is due to the distortion of the AAE conformer by crystal-field effects. This assumption does not seem to be supported by our calculations. Table 1 compares the experimental value of the CNC ring angle in RDX to the three ring angles in each of the six conformers of RDX that were predicted at the B3LYP/6-31G* level. None of the six conformers of RDX has a C−N−C ring angle of 124°. Another notable deviation of theory from experiment was seen in the value for the torsional angle ϕ used to describe the orientation of the NO_2 groups relative to the ring. As defined by Shishkov et al.,[4] $\phi = 0°$ corresponds to a geometry in which the "C...C and O...O lines of the C_2N-NO_2 fragment are coplanar". This is the value that was obtained in the B3LYP/6-31G* predictions for the AAA conformer. However, the value reported for the molecular model used by Shishkov et al.[4] is 19.1°. The two structures with different arrangements of the NO_2 groups are illustrated in Figure 1.

TABLE 1: C−N−C Ring Angles (deg) for RDX Conformers

AAE[a]	AAA[a]	twist[a]	boat[a]	EEA[a]	EEE[a]	exptl[b]AAA
115.5	115.6	116.1	117.5	117.0	117.6	123.7
115.0	115.7	114.7	117.5	117.0	117.9	
115.5	115.5	116.3	116.0	114.7	117.4	

[a] Calculated at the B3LYP/6-31G* level. [b] Reference 4.

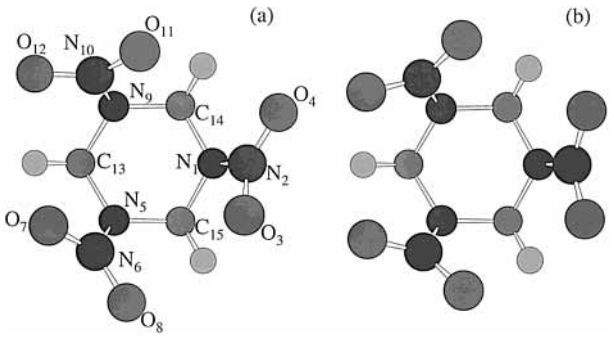

Figure 1. Structures of the AAA conformers of RDX using parameters of the (a) Shishkov et al.[4] model and (b) B3LYP/6-31G* parameters[3].

Although the electron-diffraction study[4] and ab initio study[3] that compared simulated and experimental infrared spectra conclude that the gas-phase structure is the AAA conformer, Karpowicz and Brill[8] suggested that possible low barriers to inversion of the amine nitrogens from axial to equatorial sites or substantial flexibility in the ring might produce a conformationally averaged structure. Theoretical predictions of a conformationally averaged structure would require dynamical treatments, which are beyond the scope of this study. However, we have calculated the interconversion barriers among the various conformers in order to establish whether such conformational motion might be possible at the temperatures of the experiments. We have also calculated the diffraction curves using structural information generated from ab initio calculations for all of the RDX conformers and have compared these directly to the experimental intensities. Our goal is to determine if alternative structural models to that proposed by Shishkov et al.[4] could reproduce the experimental curves.

Structural Analysis Using Electron Diffraction

Bastiansen and Skancke[10] have extensively reviewed the theory of molecular electron diffraction in the gas phase and have provided a description of the equations needed to generate electron-scattering spectra. The molecular part of the scattering

intensities, $I(s)$, is given by

$$I(s) = (Ks^{-4}) \Sigma\Sigma(Z_i - F_i)(Z_j - F_j)[\sin(r_{ij}s)/r_{ij}s] \quad (1)$$

where it is assumed that the molecule is rigid and that no phase shift occurs during the scattering process. In this equation, K is an uninteresting constant, $s = (4\pi/\lambda)\sin\theta$, λ is the wavelength of the electron, and θ is the Bragg angle (one-half of the diffraction angle). Z_i is the atomic number of ith atom, F_i is the scattering amplitude of the ith atom, and r_{ij} is the distance between the ith and jth atoms in the molecule. The sums in the above equation are taken over all atom pairs. Because molecules have thermal motion, eq 1 is corrected through the inclusion of a term that is a function of the MSAs under the assumption that the thermal motion is limited to small harmonic oscillations. The resulting expression for the molecular scattering intensities is

$$I(s) = (Ks^{-4}) \Sigma\Sigma(Z_i - F_i)(Z_j - F_j)\exp[-0.5\mu_{ij}^2 s^2] \times [\sin(r_{ij}s)/r_{ij}s] \quad (2)$$

where μ_{ij} is the mean-square amplitude (MSA) of vibration along the line connecting the ith and jth atoms. The atomic F_i values have been tabulated[11] and used in our evaluation of eq 2.

Although a general purpose molecular-orbital program such as Gaussian 98[12] can be used to calculate all of the internuclear distances and the vibrational frequencies in a molecule, these codes do not generate the MSAs that are required to calculate the scattering curves. In recent work,[13] it has been shown that the required MSAs can be easily computed using a theoretically obtained Cartesian force-constant matrix so that all of the elements are in place to calculate theoretical scattering curves for all of the RDX conformers.

Computational Details

The optimized geometries of all of the conformers reported here have been previously given.[2,3] The geometry optimizations and subsequent normal-mode analyses were recalculated in this work in order to generate the Cartesian force-constant matrixes necessary for the evaluation of the MSAs. All calculations were performed using the Gaussian 98 suite of quantum chemistry software,[12] and all calculations were subject to default settings in Gaussian 98. As in the earlier calculations,[2,3] a nonlocal DFT method using the B3LYP density functional[14,15] and the 6-31G* basis set[16] was used in all calculations. The B3LYP density functional, when used with the 6-31G* basis set, has been shown to be reasonably accurate in reproducing experimental molecular geometries.[3,17,18] Also, accurate vibrational frequencies are produced when they are scaled by 0.9613, as suggested by Wong[19] and Scott and Radom.[20] We used the approach described in ref 13 to calculate the MSAs for the six conformers of RDX at 433 K, the temperature at which the diffraction experiments were performed. The Cartesian force matrix was scaled by $(0.9613)^2$. These MSAs were used in conjunction with eq 2 to produce simulated diffraction intensity curves for six conformers of RDX. The validity of the normal-mode assumption at this temperature will be discussed in section V.

Because we are using scaled frequencies in these calculations, it is useful to understand how the MSAs change when the frequencies are scaled. The results of these calculations can be found in Table 2 for the AAA conformer of RDX. In general, as the frequencies increase, the MSAs decrease and vice versa. This simply reflects the decrease in the relative motion of the atoms with increasing vibrational frequency. It was found that the scaling of frequencies produced a range of changes in the MSAs, with smaller changes occurring for the atoms close together and larger changes occurring for atoms separated by larger distances. In absolute value, the changes in the MSAs are of the same order of magnitude as the change in the frequencies (i.e., a 5% increase in the frequencies produces 4−8% decreases in the MSAs). A 20% decrease in the frequencies, results in 9−20% increases in the MSAs. If the scale factor is assumed to reflect the error in the calculated force matrix, then the effects on the MSAs and the vibrational frequencies should be approximately the same.

TABLE 2: Effect That Scaling of Vibrational Frequencies Has on the MSAs for the AAA Conformer of RDX

frequency scaling	range of percent decrease in MSA	frequency scaling	range of percent increase in MSA
1.05	4.32 to 8.42	0.95	0.59 to 1.19
1.10	6.52 to 12.56	0.90	3.35 to 6.79
1.15	8.58 to 16.35	0.85	6.36 to 13.05
1.20	10.0 to 19.81	0.80	9.64 to 20.10

In addition to reproducing the local minima of the various conformers of RDX on the B3LYP/6-31G* surface[2,3] and evaluating their MSAs, we also located transition states connecting the various minima in order to assess whether rapid interconversion from the conformers would be likely at the temperature of the experiment (433 K). Absolute and zero-point-corrected relative energies are given in Table 3 for all of the critical points. Cartesian coordinates of all of the critical points are given in the Supporting Information. As evident in Table 3, the B3LYP/6-31G* barriers to interconversion are no greater than 5 kcal/mol.

Figure 2 illustrates the energies of the various conformers relative to the low-energy structure (AAE) and the barriers to interconversion. We estimate that the available vibrational energy for RDX at 433 K is on the order of 13 kcal/mol. According to this Figure, there is ample internal energy to cross even the barriers that involve distortions of the hexahydrotriazine ring. The EEE conformer is the high-energy conformer by over 3 kcal/mol relative to the other five, which are all within 1.26 kcal/mol of one another.

It is worth noting that the zero-point-corrected barrier leading from the EEE conformer to the EEA conformer is zero and that the difference between the uncorrected absolute energies is only 0.1 kcal/mol. Normal-mode analysis of the structure resulting from the transition-state search gave a small imaginary frequency (61i cm^{-1}). An animation of the molecular motion of this vibrational mode was consistent with the interconversion from the EEE to EEA structure. A comparison of the geometric parameters for the EEE conformer and this possible transition state revealed that the angle δ, defined by Shiskov et al.[4] as the angle between the plane of the C−N−C ring atoms and the corresponding N−N bond, differs by 10.6° between the two structures. This geometric parameter would be directly influenced by the motion of the NO_2 group in converting from EEE to EEA. It is well known that normal-mode analyses using DFT often result in nonzero frequencies on the order of 50 cm^{-1} or less for modes whose frequencies should be zero (i.e., the translational and rotational modes of the molecule).[21] These are a result of limitations associated with DFT numerical integrations.[21] Therefore, for large polyatomic molecules with internal rotors or other low-frequency motions, consideration should be given as to whether a low-frequency value corresponds to a real vibrational mode or whether the value is a result of numerical error in the calculations. For example, the smallest low-frequency "nonzero" vibrational mode in the EEE con-

TABLE 3: Absolute and Relative Energies of Critical Points on the RDX Potential Energy Surface

	type	absolute energy (hartrees)	zero-point energy[a] (kcal/mol)	relative energy[b] (kcal/mol)
		B3LYP/6-31G*		
AAE	minimum	−897.40935628	86.57	0.00
AAA	minimum	−897.40890163	86.47	0.19
twist	minimum	−897.40833809	86.69	0.76
boat	minimum	−897.40766373	86.64	1.14
EEA	minimum	−897.40724913	86.51	1.26
EEE	minimum	−897.40069314	86.12	4.99
AAA → AAE (TS1)	transition state	−897.40772117	86.37	0.82
AAE → EEA (TS2)	transition state	−897.40660005	86.38	1.53
EEA → boat (TS3)	transition state	−897.40207823	86.21	4.21
EEA→ twist (TS4)	transition state	−897.40210737	86.26	4.23
EEE → EEA	transition state	−897.40054882	86.03	4.99
		MP2/6-31G*		
AAE[c]	minimum	−895.0074868	91.76	0.00
EEE	minimum	−894.99465046	91.31	8.05
EEE → EEA	transition state	−894.99353386	91.23	9.29

[a] Frequencies are scaled by 0.9613 (see text) for all B3LYP/6-31G* structures; frequencies are unscaled for MP2/6-31G* structures. [b] Zero-point-corrected (using scaled frequencies for B3LYP/6-31G* structures); energies relative to the AAE structure. [c] Reference 3.

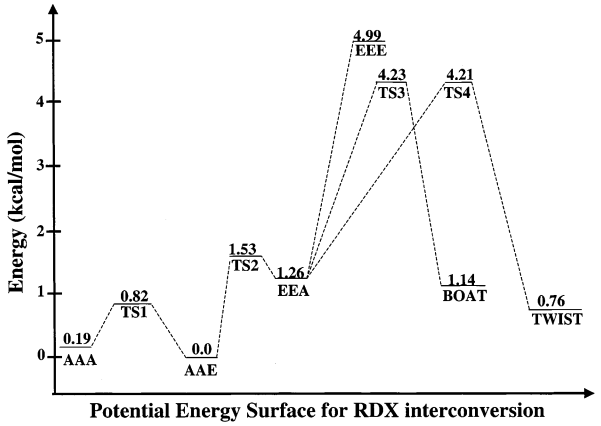

Figure 2. B3LYP/6-31G* potential energy surface for RDX interconversion. Energies are given in kcal/mol and include zero-point corrections. Labels of species correspond to those given in Table 3.

former is 44 cm^{-1}, but the normal-mode analyses also produced six zero frequencies, as expected for a critical point that corresponds to an energy minimum. Because there is a question of numerical error in the DFT calculations, we have optimized this transition state at the MP2/6-31G* level[22] to confirm whether it truly exists or is a result of numerical error in the DFT calculations. Absolute and zero-point-corrected MP2/6-31G* energies for the EEE conformer and the transition state for the EEE to EEA interconversion are given in Table 3. The results of the calculations indicate that the difference in the zero-point-corrected energies between the two critical points is only 1.24 kcal/mol at the MP2/6-31G* level, but the difference in the geometric parameter δ is more pronounced ($\Delta\delta = 28.5°$) than for the DFT structures. The frequency corresponding to the MP2 transition-state structure is 94i. Although both the DFT and MP2 calculations indicate that the barrier to converting from EEE to EEA is very small, we are assuming that the transition state is real. Nonetheless, the conversion from EEE to EEA would require a negligible amount of energy, and thus it is expected that EEE would be a transient species at 433 K.

Results and Discussion

Because the goal of this research is to explain the discrepancy in the structural parameters determined from experimental measurements and theoretical calculations, we first attempted to determine which of the conformers best represented the experimental spectrum through a direct comparison of theoretical and experimental data points. The scattering curves for the various conformers of RDX were calculated using eq 2 and are shown in Figure 3. The MSAs used in eq 2 were determined from the B3LYP/6-31G* quadratic force field in conjunction with the method described in ref 13. In this Figure, each theoretical curve is superimposed upon the experimental data provided by Shishkov et al.[4] All of the curves were normalized to the peak at $s = 27.8$ $Å^{-1}$. Also, a scattering curve assuming the structural model proposed by Shishkov et al. [4] is calculated (using eq 2) and superimposed upon the experimental data. For this curve, the structural parameters and MSAs provided in Table 1 of ref 4 were used.

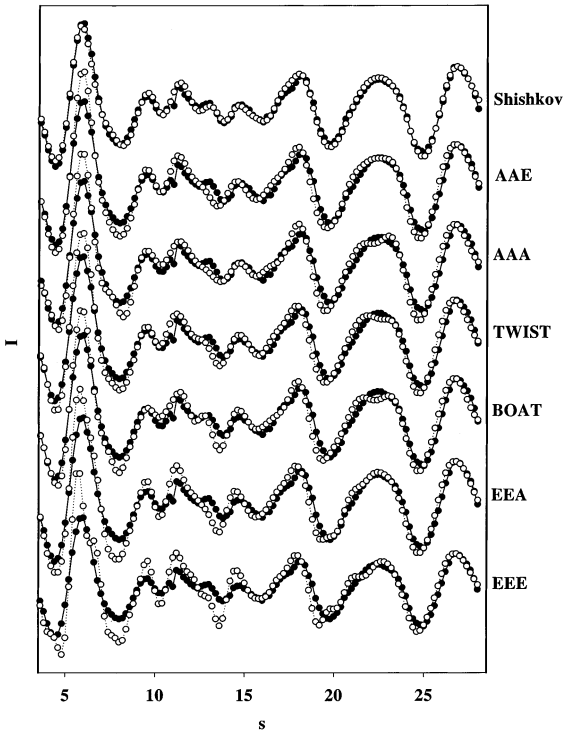

Figure 3. Experimental and theoretical molecular intensities of RDX. The molecular conformer associated with each of the theoretical curves is shown to the right of the Figure. The curve entitled "Shishkov" is the simulated spectrum using the structural model of Shishkov et al.[4].

The scattering curves for all of the conformers are remarkably similar with a few exceptions. The EEE spectrum has the poorest

TABLE 4: Structural Parameters and MSAs for RDX Molecular Models

	R(Å) or <(deg)			MSA (Å)				
		B3LYP/6-31G*			B3LYP/6-31G* structure			
					AAA		EEE	
parameter[a]	Shiskov et al.[4]	AAA	EEE	Shiskov et al.[4]	fit	calcd[b]	fit	calcd[b]
				Independent				
C−N	1.464	1.4603	1.4595	0.040	0.0108	0.0534	0.0108	0.0540
N−N	1.413	1.4226	1.4003	0.049	0.1398	0.0587	0.1398	0.0543
N═O	1.213	1.2220	1.2253	0.034	0.0633	0.0397	0.0633	0.0398
C−H	1.089	1.0901	1.0944	0.085[c]	0.0850[c]	0.0773	0.0850[c]	0.0780
NCN	109.4	112.74	105.99					
CNC	123.7	115.60	117.65					
CNN	116.3	117.46	115.44					
ONO	125.5	127.01	126.97					
HCH	105.1	110.07	109.39					
ϕ_{NN}	19.1	0.0	0.0					
				Dependent				
$O_3...O_4$	2.156	2.1872	2.1928	0.050	0.0422	0.0504	0.0329	0.0508
$N_1...O_3$	2.243	2.2503	2.2346	0.051	0.1363	0.0619	0.1433	0.0592
$N_1...N_5$	2.389	2.4318	2.3310	0.051	0.0987	0.0707	0.1494	0.0697
$C_{14}...N_2$[d]	2.443	2.4641	2.4181	0.051	0.2130	0.0709	0.1450	0.0786
$C_{13}...C_{14}$	2.582	2.4714	2.4974	0.066	0.1366	0.0723	0.1108	0.0873
$C_{15}...O_3$	2.636	2.6780	2.6152	0.109	0.2343	0.0965	0.1723	0.1166
$C_{14}...O_4$	2.698	2.6780	2.6152	0.109	0.2343	0.0965	0.1723	0.1166
$C_{13}...N_1$	2.883	2.8535	2.8199	0.085	0.1716	0.0785	0.1771	0.0817
$N_1...N_6$	3.461	3.3394	3.6119	0.102	0.1563	0.1690	0.2774	0.0825
$C_{14}...O_3$	3.493	3.5464	3.5094	0.115	0.0888	0.0746	0.0825	0.0820
$C_{15}...O_4$	3.540	3.5464	3.5094	0.115	0.0888	0.0746	0.0825	0.0820
$N_1...O_{11}$	3.646	3.5915	3.9661	0.154	0.6211	0.2338	0.1515	0.1066
$O_3...O_8$	3.908	3.2219	4.6066	0.172	0.6642	0.3799	0.6640	0.1747
$N_1...O_8$	3.911	3.5915	3.9661	0.172	0.6211	0.2338	0.1515	0.1066
$N_2...O_{11}$	3.987	3.6861	4.8384	0.172	0.3168	0.3625	0.5591	0.1343
$C_{13}...N_2$	4.090	3.9177	4.2100	0.218	0.0956	0.1693	0.1856	0.0868
$N_2...N_6$	4.182	3.7537	4.7560	0.181	0.3054	0.2960	0.6078	0.0985
$N_1...O_7$	4.262	4.2682	4.5652	0.165	0.2688	0.2117	0.2799	0.0842
$N_2...O_8$	4.401	3.6861	4.8384	0.162	0.3168	0.3625	0.5591	0.1343
$N_1...O_{12}$	4.485	4.2682	4.5652	0.096	0.2688	0.2117	0.2799	0.0842
$C_{13}...O_3$	4.591	4.5320	4.8804	0.096	0.4650	0.2300	0.4650	0.1003
$O_3...O_7$	4.800	4.7129	6.0107	0.138	0.6317	0.4652	0.6317	0.1296
$C_{13}...O_4$	4.854	4.5320	4.8804	0.163	0.4650	0.2300	0.4650	0.1003
$N_2...O_7$	4.939	4.6688	5.8170	0.163	0.6609	0.3949	0.6609	0.0957
$N_2...O_{12}$	5.277	4.6688	5.8170	0.114	0.6609	0.3949	0.6609	0.0957
$O_4...O_8$	5.589	4.7129	6.0107	0.224	0.6317	0.4652	0.6317	0.1296
$O_3...O_{12}$	5.934	5.4091	6.7991	0.259	0.5326	0.5331	0.1192	0.0980

[a] See Figure 1 for numbering of atoms. [b] Evaluated using procedure described in ref 13 and the B3LPY/6-31G* geometry and corresponding force-constant matrix. [c] Fixed parameter. [d] Carbon atom misnumbered in ref 4.

overall agreement with the experimental information, mainly in the small *s* region ($s < 15$ Å^{-1}). With the exception of the peak at $s = 13.6$ Å^{-1}, the remaining features of the experimental curve are apparent in all of the spectra associated with the six conformers. The only conformer that shows a peak at $s = 13.6$ Å^{-1} is the boat structure. The broad peak centered at $s = 22.5$ Å^{-1} is almost reproduced by the calculated curves corresponding to the AAE and EEA structures. The remaining conformers produce curves that have two peaks in this region, rather than just one.

Although each feature in the experimental spectrum is reproduced in spectra for one or more of the conformers, no single spectrum exactly reproduces all of the features of the experimental spectrum. Three possibilities could explain this discrepancy: (1) the theoretical predictions of the geometric parameters of the conformers have significant error; (2) the experimental spectrum represents a dynamically averaged structure; or (3) there are significant errors in the MSAs used to calculate the scattering intensities. We do not believe that the calculated geometry is in error because of the good agreement between the theoretical and crystalline RDX structures. As discussed in section IV, the relative energies and interconversion barriers between the conformers are low (no greater than 5 kcal/mol), indicating that at the temperature of the experiment rapid interconversion among the conformers is probable and that any measured intensities could easily reflect a dynamically averaged structure. However, the temperature of the experiment is high enough that the validity of the MSAs used in calculating the molecular scattering intensities is questionable.

Thus, we next investigated whether a simulated spectrum could be produced to match experiment using the B3LYP/6-31G* C_{3v} structures by least-squares fitting the MSAs for the models. The remaining conformers were not subjected to this fitting procedure because they do not have C_{3v} symmetry and would not have infrared vibrational spectra consistent with experimental observations.[8] As stated earlier, a molecular model was assumed in the Shishkov *et al.*[4] analysis, and both the geometric parameters and the MSAs were simultaneously varied in least-squares fitting a simulated spectrum to the measured intensities. Table 4 gives the independent and dependent geometric parameters and MSAs reported by Shishkov et al.[4] Note that the Shishkov et al.[4] model did not include any nonbonding interactions involving hydrogen. In our fitting

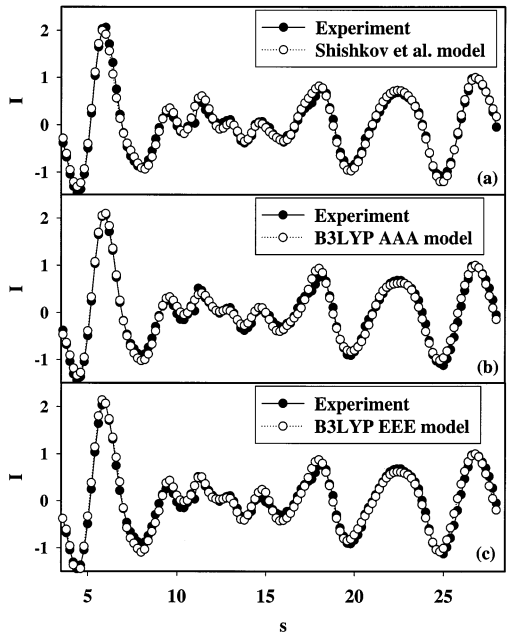

Figure 4. Theoretical molecular intensities of RDX superimposed on experimental information for (a) the structural model reported by Shishkov et al.[4], (b) the B3LYP/6-31G* AAA structure[3] using best-fit MSAs to reproduce the experimental data, and (c) the B3LYP/6-31G* EEE structure[3] using best-fit MSAs to reproduce the experimental data.

procedure, we have used a molecular model described by the same independent and dependent geometric parameters defined in Shishkov et al.[4] but whose values were fixed to those corresponding to either the B3LYP/6-31G* AAA or EEE structures. Where the theoretical geometric parameters did not conform exactly to C_{3v} symmetry, averaged values[3] were used. The MSAs resulting from this fitting procedure are given in Table 4 and compared with the values reported by Shishkov et al.[4] and the values calculated using the B3LYP/6-31G* force-constant matrixes for the C_{3v} conformers. Figure 4 shows simulated spectra, superimposed on the experimental intensities, for the Shishkov et al.[4] model (Figure 4a) and the B3LYP/6-31G* AAA and EEE models using the MSAs resulting from the least-squares fitting procedure described above (Figure 4b and c, respectively). The fitted curves reasonably reproduce the experimental information. Therefore, we have shown that alternative structures to that given in the experimental paper can be used to reproduce the measured scattering intensities.

The values of the MSAs resulting from our fitting procedure are, in most cases, significantly different from those used by Shishkov et al.[4] Likewise, several of the dependent structural parameters are significantly different, mainly because of the differences in the orientation of the NO_2 groups (see Figure 1). In the fitting procedure used by Shishkov et al.,[4] initial values of the MSAs used in their fitting procedure were consistent with those measured for similar molecules. However, Shishkov et al.[4] do not report those systems, the conditions of the experiments in which the measurements were performed, or their values. The values of the MSAs resulting from the fitting procedure are in most cases larger than those evaluated using the B3LYP/6-31G* force constant matrix, particularly for the EEE conformer. This may be an indication that the atoms in the RDX molecule are undergoing much larger motions than would be expected from simple harmonic vibrations. Because the temperature of the experiments of the RDX gas-phase molecule is 433 K, it is possible that there are significant errors in the MSAs at this temperature. The MSAs are assumed to represent small harmonic oscillations away from the equilibrium distances, which would be expected at low temperatures. The accuracy of the calculated values is completely dependent on the soundness of the normal-mode approximation at this temperature. Also, Baistiansen and Skancke[10] clearly indicate that the validity of the expressions used to represent the molecular scattering (eqs 1 and 2) is dependent on appropriate thermal corrections to the assumption of rigid molecules. Anharmonic effects could be quite large for a molecule such as RDX because it has several low-frequency modes involving the interconversion of the ring and the rotational motions of the NO_2 groups. These effects would produce larger MSAs than would be calculated on the basis of simple harmonic motions of the atoms about their equilibrium positions. Thus, we think a significant source of error in the simulated spectra might lie in the values of the MSAs.

Conclusions

To investigate discrepancies in molecular structural information generated through ab initio calculations and an analysis of electron-diffraction data, we have generated diffraction intensity curves using DFT for six conformers of RDX. The curves were generated using molecular structure information and MSAs of vibration along the lines between atoms in the conformers. The MSAs were calculated from the Cartesian force-constant matrixes generated at the B3LYP/6-31G* level of theory. Each feature in the experimental spectrum is reproduced in one or more of the conformers; however, none of the individual spectra completely matched each feature in the experimental spectrum. Because of the temperature at which the experiments were undertaken, however, there is a question as to the validity of the use of the MSAs in the equations describing the molecular scattering intensities, which assume small harmonic oscillations of the atoms from the equilibrium positions.

Spectra were generated assuming the B3LYP/6-31G* AAA and EEE structures, using MSAs that were varied in a least-squares fitting procedure to reproduce the experimental information. The resulting curves are in reasonable agreement with the experiment, indicating that alternative structures could be used to reproduce the experimental spectrum.

Finally, barriers to interconversion among the conformers were calculated and shown to be no larger than 5 kcal/mol. These calculations were performed to investigate the proposal of Karpowicz and Brill[8] that the structure in the gas phase (and in solution) is a conformationally averaged structure consisting of contributions from rapidly interconverting species. The similarity in the spectra for the various conformers, possible error in the MSAs, and the low interconversion barriers may be partly responsible for making this experiment difficult to interpret. If more than one conformer exists in equilibrium in the gas phase, then the interpretation of these data on the basis of only one conformer could easily lead to geometric distortions that would compensate for the contributions of the conformers that were not included in the analysis. The interpretation of the experimental data on the basis of several conformers in equilibrium would be more difficult because many more geometric parameters would have to be determined. In this case, we have shown that for RDX, alternative structures (i.e., one with a different set of geometric parameters or one that is a conformationally averaged structure) cannot be precluded from the analysis used in determining the structure of RDX in the gas phase. This study clearly illustrates how modern computational methods can complement interpretations of difficult experiments.

Acknowledgment. We thank Professor I. F. Shishkov, Moscow State University, for providing the measured electron-diffraction intensities for RDX. All calculations were performed at the Army Research Laboratory Major Shared Resource Center, Aberdeen Proving Ground, Maryland.

Supporting Information Available: Cartesian coordinates of all of the critical points. This material is available free of charge via the Internet at http://pubs.acs.org.

References and Notes

(1) Traetteberg, M.; Richardson, A. D.; Hedberg, K.; Winter, R. W.; Gard, G. L. *J. Phys. Chem. A* **2001**, *105*, 9587.
(2) Harris, N. J.; Lammertsma, K. *J. Am. Chem. Soc.* **1997**, *119*, 6583.
(3) Rice, B. M.; Chabalowski, C. F. *J. Phys. Chem. A* **1997**, *101*, 8720.
(4) Shishkov, I. F.; Vilkov, L. V.; Kolonits, M.; Rozsondai, B. *Struct. Chem.* **1991**, *2*, 57.
(5) Harris, P. M.; Reed, P. Technical Report AFOSR-TR-59-165; Ohio State University Research Foundation: Columbus, OH, 1959.
(6) Choi, C. S.; Prince, E. *Acta Crystallogr., Sect. B* **1972**, *28*, 2857.
(7) Filhol, A.; Clement, C.; Forel, M.-T.; Paviot, J.; Rey-Lafon, M.; Richoux, G.; Trinquecoste C.; Cherville, J. *J. Phys. Chem.* **1971**, *75*, 2056.
(8) Karpowicz, R. J.; Brill, T. B. *J. Phys. Chem.* **1984**, *88*, 348.
(9) Iqbal, Z.; Suryanarayanan, K.; Bulusu, S.; Autera, J. R. Technical Report No. 4401; Picatinny Arsenal: Dover, NJ, October 1972.
(10) Bastiansen, O.; Skancke, P. N. *Adv. Chem. Phys.* **1961**, *3*, 323.
(11) *International Tables for X-ray Crystallography*; Ibers, J. A., Hamilton, W. C., Ed.; The Kynoch Press: Birmingham, England, 1974; p 176.
(12) Frisch, M. J.; Trucks, G. W.; Schlegel, H. B.; Scuseria, G. E.; Robb, M. A.; Cheeseman, J. R.; Zakrzewski, V. G.; Montgomery, J. A., Jr.; Stratmann, R. E.; Burant, J. C.; Dapprich, S.; Millam, J. M.; Daniels, A. D.; Kudin, K. N.; Strain, M. C.; Farkas, O.; Tomasi, J.; Barone, V.; Cossi, M.; Cammi, R.; Mennucci, B.; Pomelli, C.; Adamo, C.; Clifford, S.; Ochterski, J.; Petersson, G. A.; Ayala, P. Y.; Cui, Q.; Morokuma, K.; Malick, D. K.; Rabuck, A. D.; Raghavachari, K.; Foresman, J. B.; Cioslowski, J.; Ortiz, J. V.; Stefanov, B. B.; Liu, G.; Liashenko, A.; Piskorz, P.; Komaromi, I.; Gomperts, R.; Martin, R. L.; Fox, D. J.; Keith, T.; Al-Laham, M. A.; Peng, C. Y.; Nanayakkara, A.; Gonzalez, C.; Challacombe, M.; Gill, P. M. W.; Johnson, B. G.; Chen, W.; Wong, M. W.; Andres, J. L.; Head-Gordon, M.; Replogle, E. S.; Pople, J. A. *Gaussian 98*, revision A.7; Gaussian, Inc.: Pittsburgh, PA, 1998.
(13) Vladimiroff, T. *J. Mol. Struct.: THEOCHEM* **2000**, *507*, 111.
(14) Becke, A. D. *Phys. Rev. A: At., Mol., Opt. Phys.* **1988**, *38*, 3098. Becke, A. D. *J. Chem. Phys.* **1993**, *98*, 5648.
(15) Lee, C.; Yang, W.; Parr, R. G. *Phys. Rev. B* **1988**, *37*, 785.
(16) Hariharan, P. C.; Pople, J. A. *Theor. Chim. Acta* **1973**, *28*, 213.
(17) Bauschlicher, C.W., Jr. *Chem. Phys. Lett.* **1995**, *246*, 40.
(18) Vladimiroff, T. *J. Mol. Struct.: THEOCHEM* **1998**, *453*, 119.
(19) Wong, M. W. *Chem. Phys. Lett.* **1996**, *256*, 391.
(20) Scott, A. P.; Radom, L. *J. Phys. Chem.* **1996**, *100*, 16502.
(21) Ochterski, J. W. *Vibrational Analysis in Gaussian;* http://www-.Gaussian.com/vib.htm#SECTION00050000000000000000; October 29, 1999.
(22) Moeller, C.; Plesset, M. S. *Phys Rev.* **1934**, *46*, 618.